Hydrodynamics of liquid crystals using a Maier-Saupe free energy

Lucas Myers

May 2, 2022

1 Introduction

Nematic liquid crystals constitute an interesting phase between crystals and typical fluids because they exhibit orientational order, but lack translational order. Thus their molecules tend to orient themselves along the same axis for thermodynamic reasons, but their evolution is also mediated by flows throughout the system. Further, topological defects can arise when molecular orientations wrap around points or lines in nontrivial ways. It is a considerable challenge to properly couple both the thermodynamic effects of alignment with the hydrodynamic flow effects, especially when the topological nature of defects makes it necessary to introduce a tensor-valued order parameter to keep track of the liquid crystal state. Here we describe one of the previously-proposed hydrodynamic models, and adjust the bulk free energy so that the model can describe anisotropic elasticity – that is, a system in which different types of molecular distortions are preferred differently by the system.

To begin, we give an introduction to liquid crystal theory, first in the equilibrium case and then in the non-equilibrium case describing both the typical Landau-de Gennes free energy, and then the somewhat lesser-used Maier-Saupe mean-field free energy. After this we introduce the hydrodynamic model, and subsequently show the computational scheme which is used to solve the model. To establish the efficacy of our code, we compare configurations prepared by our computational scheme to other, previously-established results. Finally, we indicate some of the systems and phenomena which we hope to investigate with our model.

2 Equilibrium liquid crystal theory

2.1 The Q-tensor

The systems that we will be concerned with display nematic liquid crystal phases. The phrase "liquid crystal" indicates that the molecules lack positional order like a liquid, but they have strong orientational order like a crystal. Put another way, the molecules are able to move around one another with relative ease, but they tend to align along some preferred direction. To display this kind of aligning behavior, the molecules in question must be anisotropic in some way. In 1, the molecule is completely anisotropic and so we may assign a vector roughly along its longest axis, and pointing in some particular direction (here we choose towards the benzene rings, but we could have just as easily chosen towards the tail).

Now, these types of molecules tend to have three types of purely orientational patterns: polar, nematic, or isotropic – some form spatial patterns, but we neglect those here. Schematics of these alignment types are given in 2
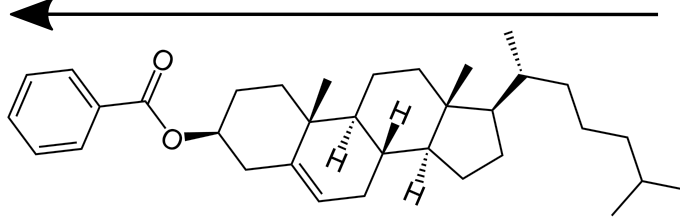
Figure 1: A cholesteryl benzoate molecule, along with an arrow representing a unit vector which we use to characterize its orientation. Image from (REFERENCE WIKIMEDIA COMMONS)
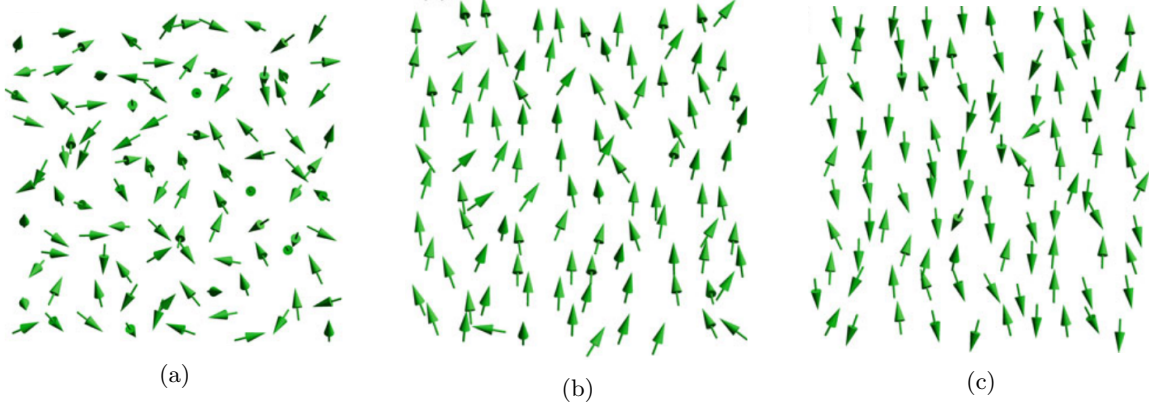

(a)

(b)

(c)

Figure 2: Schematic representation of (a) isotropic, (b) polar, and (c) nematic alignment patterns of molecules. Cartoons taken from (REFERENCE SELINGER)

In short, polar alignment refers to molecules all pointing the same direction, nematic to molecules pointing along the same axis but not necessarily along the same direction, and isotropic to molecule orientations being uniformly distributed. In the same way that total magnetization characterizes the state of a two-state spin system in the Ising model, we would like to characterize our system state with a relatively simple object (order parameter) so that we do not have to list off the individual molecular orientations to say something about our system. In particular we want to differentiate between nematic and isotropic states – for our purposes polar states may be ignored.

As a first guess, we could follow the Ising model as closely as possible and just take an average over the orientations:

$$M = \langle r \rangle$$

where here r is a unit vector assigned to each molecule as in 1 In the isotropic case this evaluates to zero for all components since, in the limit of large system size, for any particular molecule with orientation r we will be able to find another molecule with orientation $-r$. However, for the case of a perfect nematic pointing along (without loss of generality) the $\pm z$-axis, for each molecule with orientation $(0, 0, 1)$ there will be a corresponding molecule with orientation $(0, 0, -1)$. Hence, our vector average cannot distinguish between isotropic and nematic phases. Indeed, a little thought would have shown us that this scheme was doomed from the start, because both of these states have some kind of reflection symmetry about some axis, and so any quantity that is odd in the orientation vector will give us zero. Instead, we must make a product of the orientation vector with itself so that the quantity is even. Clearly the standard dot and cross products will not work, because the former always gives 1 (since the orientation vector is a unit vector) and the latter gives zero. Hence, we may instead use the *tensor* product to define a tensor-valued order parameter:

$$T = \langle r \otimes r \rangle \tag{1}$$

In the isotropic case, we must have that $\langle r_x^2 \rangle = \langle r_y^2 \rangle = \langle r_z^2 \rangle$ essentially by definition of the isotropic state. Further, we have that:

$$\langle r \cdot r \rangle = \langle r_x^2 \rangle + \langle r_y^2 \rangle + \langle r_z^2 \rangle = 1 \tag{2}$$

Hence the diagonal elements are just $1/3$. Additionally, for the off-diagonal elements in the thermodynamic limit, for every vector (r_x, r_y, r_z) we may find a corresponding $(r_x, r_y, -r_z)$ which will cancel out in the average. Hence the off-diagonal is zero so that:

$$T^{\text{iso}} = \begin{pmatrix} \frac{1}{3} & 0 & 0 \\ 0 & \frac{1}{3} & 0 \\ 0 & 0 & \frac{1}{3} \end{pmatrix} \tag{3}$$

In the case of a perfectly ordered system, say along the z-axis so that $r = (0, 0, \pm 1)$, we may explicitly calculate this tensor as:

$$T^{\text{nem}} = \begin{pmatrix} 0 & 0 & 0 \\ 0 & 0 & 0 \\ 0 & 0 & 1 \end{pmatrix} \tag{4}$$

To find the order parameter for a system oriented along any other axis, we may just apply a rotation matrix which rotates the z-axis to the r-axis. In any case, it is clear that we may distinguish between a completely nematically ordered state and an isotropic state.

Now we make an addition to make this tensor more mathematically tidy. Clearly this tensor is symmetric, and the trace is always 1 since it is the average of the dot product. By adding another symmetric tensor whose trace is -1, we may create a traceless and symmetric order parameter, which explicitly reduces our degrees of freedom to, at most, 5 and is more desireable mathematically. Hence, we define:

$$Q = \langle r \otimes r \rangle - \frac{1}{3} I \tag{5}$$

with I the 3×3 identity matrix.

One final comment on the number of degrees of freedom of Q and how they relate to the properties of the nematic system: One might intuitively think that we only need 3 degrees of freedom to describe the system – two for the average molecular orientation, and one to describe the amount of order (i.e. how isotropic vs. ordered the system is). However, as stated above Q has 5 degrees of freedom. To see what's going on here, note that we may diagonalize the tensor into an orthonormal eigenbasis with eigenvalues $\{q_1, q_2, -(q_1 + q_2)\}$ and corresponding eigenvectors $\{n, m, l\}$:

$$Q = q_1(n \otimes n) + q_2(m \otimes m) - (q_1 + q_2)(l \otimes l) \tag{6}$$

Now, in the eigenbasis we have that $n \otimes n + m \otimes m + l \otimes l = I$ which is, in fact, basis independent. Hence we may add and subtract $\frac{1}{2} q_1 I$ to our expression to get:

$$Q = \tfrac{3}{2} q_1(n \otimes n - \tfrac{1}{3} I) + (\tfrac{1}{2} q_1 + q_2)(m \otimes m) - (\tfrac{1}{2} q_1 + q_2)(l \otimes l) \tag{7}$$

Defining $S = \frac{3}{2} q_1$, and $P = \frac{1}{2} q_1 + q_2$ we explicitly see our five degrees of freedom:

$$Q = S(n \otimes n - \tfrac{1}{3} I) + P(m \otimes m - l \otimes l) \tag{8}$$

Here S and P are independent parameters, n is defined by a polar angle and an azimuthal angle, m is defined by a single angle in the plane perpendicular to n, and l is completely determined.

If we consider eq. (5), for a set of particles that is uniformly distributed in the azimuthal direction about a main axis n, then we may write each molecule as:

$$r = m \cos \phi \sin \theta + l \sin \phi \sin \theta + n \cos \theta \tag{9}$$

3

We call these types of systems "uniaxial" because the molecules point mainly along one axis. If we calculate $\langle r \otimes r \rangle - \frac{1}{3}I$, we get:

$$\langle r \otimes r \rangle - \tfrac{1}{3}I = \left(\langle \cos^2 \theta \rangle - \tfrac{1}{3} \right) n \otimes n + \left(\tfrac{1}{2} \langle \sin^2 \theta \rangle - \tfrac{1}{3} \right) m \otimes m + \left(\tfrac{1}{2} \langle \sin^2 \theta \rangle - \tfrac{1}{3} \right) l \otimes l$$
$$= \left\langle \cos^2 \theta - \tfrac{1}{3} \right\rangle n \otimes n - \tfrac{1}{2} \left\langle \cos^2 \theta - \tfrac{1}{3} \right\rangle m \otimes m - \tfrac{1}{2} \left\langle \cos^2 \theta - \tfrac{1}{3} \right\rangle l \otimes l \tag{10}$$

where any term with $\cos \phi$ or $\sin \phi$ has gone to zero, and any term with $\sin^2 \phi$ or $\cos^2 \phi$ has gone to $\frac{1}{2}$. Now we may simply read off the eigenvalues of Q to find that:

$$S = \tfrac{3}{2} \langle \cos^2 \theta - \tfrac{1}{3} \rangle = \langle P_2(\cos \theta) \rangle \tag{11}$$

where P_2 is the second Legendre polynomial. Hence, if $S = 1$ we have that $\theta = 0$ always which corresponds to perfect alignment. Otherwise, if θ is uniformly distributed we have that $S = 0$. Thus, S characterizes the degree of alignment and n – sometimes called the "director" – characterizes the direction of alignment in uniaxial nematics. Indeed, historically the development of liquid crystal theory has used the director formalism heavily and we will refer to this formalism often.

2.2   Landau-de Gennes free energy

To predict the equilibrium configuration of a liquid crystal system, we must first write down a free energy as a function of the order parameter, and then find the order parameter value which minimizes this free energy. As a first approach, we recount the method elucidated by Landau and applied to nematic liquid crystal systems by de-Gennes. This is done by first assuming that the free energy is a smooth function, and then Taylor expanding in the appropriate order parameter, in this case the Q-tensor. Additionally, we only keep terms which obey the symmetry of the system. For us, these are terms which can undergo an arbitrary rotation, given that the direction of alignment will correspond to a broken symmetry when the phase transitions from the isotropic state to the nematic state.

Given that we have a tensor-valued order parameter, the terms which are unchanged by rotations are all of the possible ways the Q-tensor can be contracted to get a scalar value. In order to see a first-order phase transition from isotropic to nematic phases, one must expand up to fourth order in Q:

$$F(Q) = \frac{1}{2}A(Q:Q) + \frac{1}{3}B(QQ):Q + \frac{1}{4}C_1(Q:Q)^2 + \frac{1}{8}C_2(QQ):(QQ) \tag{12}$$

where here juxtaposition means standard matrix multiplication $QQ \to Q_{ik}Q_{kj}$, and dots indicate contraction over indices from innermost to outermost $Q:Q \to Q_{ij}Q_{ji}$. $A, B, C_1,$ and C_2 are all imperical quantities. Note that:

$$(Q:Q)^2 = 2(QQ):(QQ) \tag{13}$$

which can be seen most easily by choosing a basis wherein Q is diagonal (both quantities are scalar and are therefore unchanged by rotations), and then explicitly calculating the contractions. Given this, we can define $C = (C_1 + \frac{1}{2}C_2)$ to get only three terms in our free energy:

$$F(Q) = \frac{1}{2}A(Q:Q) + \frac{1}{3}B(QQ):Q + \frac{1}{4}C(Q:Q)^2 \tag{14}$$

For a uniaxial nematic $(P = 0)$ the free energy only depends on the scalar order parameter S, given that it must be insensitive to rotations. A is typically taken to be linear in temperature for thermotropic liquid crystals $A = a(T - T_0)$ with T_0 some reference temperature, and so we plot the free energy for several values of A which corresponds to several temperatures in 3a.

At low temperatures, the global minimum is at $S \neq 0$ so that the system is in a nematic state, whereas at high temperatures the global minimum is at $S = 0$, the isotropic state. There is a cross-over at $A = A_{IN}$ at which point we have a coexistence region between isotropic and nematic phases. Thus, the theory correctly predicts a phase change, supposing that the empirical parameters have the correct signs.
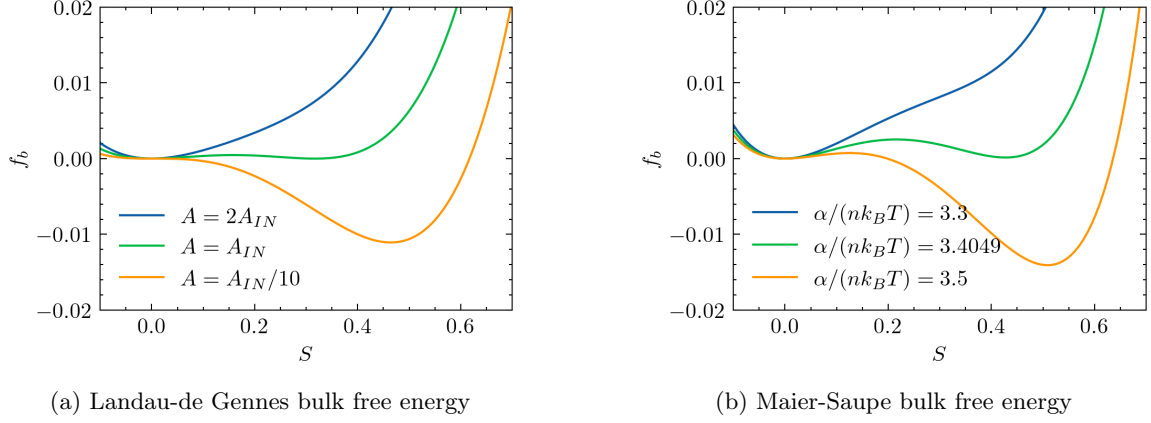
4

(a) Landau-de Gennes bulk free energy   (b) Maier-Saupe bulk free energy

Figure 3: Landau-de Gennes and Maier-Saupe bulk free energies as a function of the scalar order parameter S for a uniaxial system. For LdG we vary the A parameter in terms of A_{IN}, and for MS we vary α/nk_BT around 3.4049, both being the value at which the isotropic-nematic transition occurs.

2.3 Maier-Saupe mean-field energy

While the Landau approach works for many systems, and is rather powerful given its relative simplicity, we seek a theory which is more grounded in the microscopic details of the system. This will allow us to write a theory which has far fewer undetermined factors such as the A, B, C of Landau-de Gennes, as well as avoid some pitfalls when we venture into nonequilibrium thermodynamics in 3.

To begin, we write down an average energy corresponding to the nematic system which will then help us write down a free energy. Rather than trying to enumerate the average energy from pairwise interactions between particles, we make a mean-field approximation whereby each molecule interacts with an effective potential produced by all other molecules. In this way, we can uncouple fluctuations of individual molecules, and thus neglect correlations between their orientations.

To start, we assume that the pair-wise particle energy of the liquid crystal molecules is only dependent on relative angle γ get:

$$U = -J P_2 \cos(\gamma) = -J \left[\frac{3}{2} \cos^2(\gamma) - \frac{1}{2} \right] \tag{15}$$

Here $J > 0$ so that the energy is minimized when γ is a multiple of π (i.e. the particles are aligned or antialigned). One may derive this potential in any number of ways, including a quantum mechanical calculation of the dipole interactions between particles, an excluded volume calculation by treating the particles as cylinders, or by taking the pairwise energy as an arbitrary function of orientation and expanding in spherical harmonics. In any case, we may use this interaction potential along with the mean-field approximation to derive an average energy for the system:

$$\langle E \rangle = -\alpha Q_{ij} Q_{ji} \tag{16}$$

with $\alpha = \frac{1}{3} N q J$ where N is the number of molecules, and q is the number of neighbors that each particle interacts with. For calculation details, see Appendix A.

Now that we have an energy as a function of the order parameter, we must write down a free energy. This is done in the usual way, using the definition of the free energy in terms of the entropy:

$$F = \langle E \rangle - T S_{\text{entropy}} \tag{17}$$

where

$$S_{\text{entropy}} = n k_B \int_{S^2} p(\xi) \log\left(4\pi p(\xi)\right) d\xi \tag{18}$$

5

where the probability distribution function $p(\xi)$ describes the probablility that a particular molecule be pointing in some direction given by a point ξ on the unit sphere S^2, and n is the number density of the molecules. Note that, because the interaction energy only depends on the relative angle modulo π, we have that $p(\xi) = p(-\xi)$.

To determine S as a function of the order parameter Q, we first consider its definition in terms of the probability distribution:

$$Q = \int_{S^2} \left(\xi \otimes \xi - \tfrac{1}{3}I\right) p(\xi)d\xi \tag{19}$$

Given that there are many potential $p(\xi)$ functions which will produce a particular value for Q, we seek the one which will maximize S. This may be done via the method of Lagrange multipliers, by first fixing a value of Q and then taking (19) to be a constraint on $p(\xi)$. The resulting Lagrangian is given as:

$$\begin{aligned}
\mathcal{L}[p] &= S_{\text{entropy}} - \Lambda : \left(\int_{S^2} \left(\xi \otimes \xi - \tfrac{1}{3}I\right) p(\xi)d\xi - Q\right) \\
&= \int_{S^2} p(\xi) \left(nk_B \log\left(4\pi p(\xi)\right) - \Lambda : (\xi \otimes \xi - \tfrac{1}{3}I)\right) d\xi - \Lambda : Q
\end{aligned} \tag{20}$$

where Λ is a tensorial Lagrange multiplier. Note that (19) actually only defines five constraints, because the fixed Q will be traceless and symmetric by definition, and the integral around the sphere has a traceless and symmetric integrand regardless of $p(\xi)$. Hence, if $p(\xi)$ satisfies the five constraints corresponding to the five degrees of freedom of Q then it will necessarily satisfy the other (redundant) constraints. For the sake of finding a unique set of Lagrange multiplier values, we then take Λ to also be traceless and symmmetric so that only the unique constraint equations show up in (20).

To maximize the Lagrangian, we take the variation, which yields:

$$\delta\mathcal{L} = \int_{S^2} \left(nk_B \log\left(4\pi p(\xi)\right) - \Lambda : (\xi \otimes \xi - \tfrac{1}{3}I) + nk_B\right) \delta p \, d\xi \tag{21}$$

For the above to be zero for an arbitrary variation δp, we must have that the factor in parentheses is zero. Solving the expression for $p(\xi)$ yields:

$$p(\xi) = \frac{1}{4\pi} \exp\left(-\left(\frac{1}{nk_B}\frac{1}{3}\Lambda : I + 1\right)\right) \exp\left(\frac{1}{nk_B}\Lambda : (\xi \otimes \xi)\right) \tag{22}$$

We have one further restriction on $p(\xi)$, which is that it integrates to one. Dividing by its integral around the sphere cancels the factors out front which are constant in ξ. Further, we redefine $\Lambda \to nk_B\,\Lambda$, so that the expression simplifies to:

$$p(\xi) = \frac{\exp\left(\xi^T \Lambda\, \xi\right)}{Z[\Lambda]} \tag{23}$$

with the partition function $Z[\Lambda]$:

$$Z[\Lambda] = \int_{S^2} \exp\left(\xi^T \Lambda\, \xi\right) d\xi \tag{24}$$

Note that we have used the identity $\Lambda : (\xi \otimes \xi) = \xi^T \Lambda\, \xi$ which is a simple computation using Cartesian coordinates.

Given this, we may find Λ implicitly as a function of Q from (19):

$$\begin{aligned}
Q &= \frac{1}{Z} \int_{S^2} \exp(\xi^T \Lambda\, \xi) \left(\xi \otimes \xi - \tfrac{1}{3}I\right) d\xi \\
&= \frac{\partial \log Z}{\partial \Lambda} - \frac{1}{3}I
\end{aligned} \tag{25}$$

6

where we have integrated the second term using the definition of Z. Additionally, we have an explicit expression for S_{entropy} in terms of the Lagrange multiplier Λ:

$$\begin{aligned} S_{\text{entropy}} &= nk_B \frac{1}{Z} \int_{S^2} \exp(\xi^T \Lambda \, \xi) \left(\log 4\pi + \xi^T \Lambda \, \xi - \log Z \right) d\xi \\ &= nk_B \left(\log 4\pi - \log Z + \Lambda : \left(Q + \tfrac{1}{3} I \right) \right) \end{aligned} \tag{26}$$

where we have again used the definition of Z and expression for Q to compute the integrals.

Supposing that we may invert (25) – we will do this numerically in section 5 – we have an expression for the free energy in terms of Q. Given that the free energy is a scalar, it is rotationally invariant and so for a uniaxial system ($P = 0$) the free energy should only be a function of the scalar order parameter S. We plot the free energy below for three different temperatures in 3b For high temperatures, we see there is one minimum at $S = 0$ which corresponds to an isotropic state. At lower temperatures, there is one minimum at $S > 0$ which corresponds to a (partially) nematically ordered state. At some critical temperature T_C, we see that there are two minima, one at $S = 0$ and one at $S > 0$ at which point the isotropic and nematic phases can coexist. Again, the theory correctly predicts a phase transition, but has far fewer undetermined parameters, and will also be able to handle a wider variety of systems.

3 Nonequilibrium dynamics

3.1 Maier-Saupe field theory

To extend the model to the case of nonequilibrium dynamics, we use the field theory presented in (cite Majumdar) wherein the order parameter is assumed to be in local equilibrium over a small volume at every point in space. In this case, Λ also becomes a function of position, and the free energy becomes a free energy density which must be integrated over space:

$$f_b = -\alpha Q : Q - nk_B T \left(\log 4\pi - \log Z + \Lambda : \left(Q + \tfrac{1}{3} I \right) \right) \tag{27}$$

Here we have labeled the free energy density to indicate that it corresponds to a *bulk* free energy.

To account for spatial variation in the order parameter field over the domain, we must introduce elastic terms to the free energy density. The standard way of going about this for a uniaxial nematic with a fixed scalar order parameter S is to write down all possible gradients in the director field up to second order which are invariant under spatial rotations and sign change of the director. The result consists of four terms (supposing molecules are achiral), called the Frank elastic terms. In general, these have four different associated elastic constants K_1, K_2, K_3, K_4 which correspond to splay, twist, bend, and saddle-splay distortions of the director field respectively – see Fig. 4 for a visualization of the first three of these modes.

It happens that K_4 is a divergence of a field, and so can be reduced to a surface integral by the divergence theorem. For now we fix the configuration at the boundaries (Dirichlet conditions) and so the saddle-splay term is inconsequential for our model.

To extend this these terms to a tensor theory, we consider the possible invariants which involve gradients of the Q-tensor, and then use those which reduce to the Frank elastic terms in the case of a uniaxial, constant scalar-order nematic. These are as follows:

$$f_e(\nabla Q) = L_1 \left| \nabla Q \right|^2 + L_2 \left| \nabla \cdot Q \right|^2 + L_3 \nabla Q \vdots \left[(Q \cdot \nabla) \, Q \right] \tag{28}$$

In index notation this reads:

$$f_e(Q, \nabla Q) = L_1 \left(\partial_k Q_{ij} \right)^2 + L_2 \left(\partial_j Q_{ij} \right)^2 + L_3 Q_{lk} \left(\partial_l Q_{ij} \right) \left(\partial_k Q_{ij} \right) \tag{29}$$
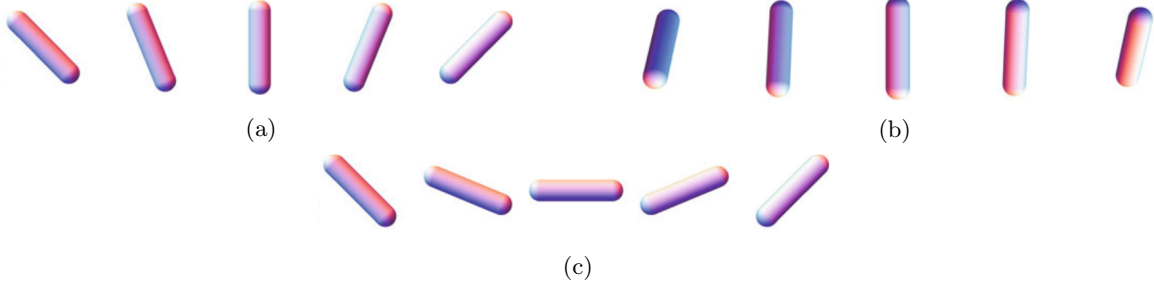
7

(a)

(b)

(c)

Figure 4: A cartoon of different possible gradients that the director can undergo. In (a) splay, the gradient direction points perpendicular to the main director component, but parallel to the varying component. In (b) twist, the gradient direction points perpendicular to the main director component, and perpendicular to the varying component. In (c) bend, the gradient direction is parallel to the main director component and perpendicular to the varying component. This figure is taken from (REFERENCE SELINGER).

These elastic constants may be written in terms of the Frank elastic constants and the constant scalar order parameter. Note that, given the added freedom of a tensorial order parameter to capture nonuniform order and biaxiality, there are much more complicated theories that one may write down in principle.

For our simplified system, the total free energy is then given by an integral of the free energy densities over the domain:

$$F = \int_\Omega f_b(Q) + f_e(Q, \nabla Q)dV = \int_\Omega f(Q, \nabla Q)dV \tag{30}$$

Then, for a purely thermodynamically-driven system, the time evolution of the order parameter can be found by taking the negative variation of the free energy with respect to the order parameter:

$$
\begin{aligned}
-\delta F &= -\int_\Omega \left(\frac{\partial f}{\partial Q}\delta Q + \frac{\partial f}{\partial(\nabla Q)}\delta(\nabla Q) \right) dV \\
&= -\int_\Omega \left(\frac{\partial f}{\partial Q} - \nabla \cdot \frac{\partial f}{\partial(\nabla Q)} \right) \delta Q \, dV
\end{aligned}
\tag{31}
$$

The time evolution of the order parameter field is then the traceless, symmetric part of the factor in parentheses:

$$\frac{\partial Q}{\partial t} = -\frac{\partial f}{\partial Q} + \nabla \cdot \frac{\partial f}{\partial(\nabla Q)} \tag{32}$$

In order so maintain the traceless and symmetric character of Q, we must introduce a Lagrange multiplier scheme which adds the following constraints to the free energy:

$$f_l(Q) = \lambda_0 Q : I + \lambda \cdot (\varepsilon : Q) \tag{33}$$

where λ_0 is a scalar Lagrange multiplier enforcing Q be traceless, λ is a vector Lagrange multiplier enforcing Q be symmetric, and ε is the Levi-Civita tensor.

An explicit calculation of the time evolution yields:

$$
\begin{aligned}
\frac{\partial Q}{\partial t} = {}& 2\alpha Q - nk_B T\Lambda + 2L_1 \nabla^2 Q \\
& + L_2 \left(\nabla(\nabla \cdot Q) + [\nabla(\nabla \cdot Q)]^T - \tfrac{2}{3}(\nabla \cdot (\nabla \cdot Q))I \right) \\
& + L_3 \left(2\nabla \cdot (Q \cdot \nabla Q) - (\nabla Q):(\nabla Q)^T + \tfrac{1}{3}|\nabla Q|^2 I \right)
\end{aligned}
\tag{34}
$$

This is the purely thermodynamic time-evolution equation for the order parameter Q.

8

3.2 Landau-de Gennes and anisotropic elasticity

A typical approximation that is used when modeling nematic liquid crystals is that elasticity is isotropic: that is, each of the deformation modes shown in Fig. 4 are penalized by the same amount in the free energy. More concretely, $K_1 = K_2 = K_3 = K_4$ which translates, in the tensorial picture, to $L_2 = L_3 = 0$. However, this is is not always a valid approximation. For example, in an actin-based nematic liquid crystal system, it has been shown that the ratio of bend to splay constants K_3/K_2 can be varied from about 0.5 to 2 by varying the filament length, which drastically changes the defect shape [3]. This poses a problem, because for a fourth order Landau-de Gennes bulk free energy as given in 14, and an elastic free energy as given by 28 with $L_3 \neq 0$, one is able to make the free energy arbitrarily large and negative. Hence, there is no global minimizer of the free energy functional, and so the evolution of such systems is liable to blow up.

To elucidate this, we do a short calculation on a simple system. Consider a nonequilibrium Q-configuration given by:

$$Q = (S_0 + \epsilon \sin(kx)) \operatorname{diag}(q_1, q_2, q_3) \tag{35}$$

Here the director points in a fixed direction along the x-, y-, or z-axis dictated by eigenvalues q_1, q_2, q_3, and varies periodically in the scalar order parameter according to S_0, ϵ, and k. Calculating the bulk free energy density yields:

$$
\begin{aligned}
f_b(Q) = (S_0 + \epsilon \sin(kx))^2 \Big[&\tfrac{A}{2} \left(q_1^2 + q_2^2 + q_3^2 \right) \\
&+ \tfrac{B}{3} \left(S_0 + \epsilon \sin(kx) \right) \left(q_1^3 + q_2^3 + q_3^3 \right) \\
&+ \tfrac{C}{4} \left(S_0 + \epsilon \sin(kx) \right)^2 \left(q_1^2 + q_2^2 + q_3^2 \right)^2 \Big]
\end{aligned}
\tag{36}
$$

while the elastic free energy density yields:

$$f_e(Q, \nabla Q) = \left[L_1 + L_3 q_1 \left(S_0 + \epsilon \sin(kx) \right) \right] \epsilon^2 k^2 \left(q_1^2 + q_2^2 + q_3^2 \right) \cos^2(kx) \tag{37}$$

Clearly k does not control the amplitude in 36, and will thus not affect the total bulk free energy of a configuration, supposing the free energy density is integrated over some integer number of oscillations. However, from 37 the total elastic free energy is quadratic in k. Hence, so long as we have that:

$$L_3 q_1 (S_0 + \epsilon \sin(kx)) < -L_1 \tag{38}$$

on a majority of the domain, then k can increase without bound to give a total free energy that is arbitrarily negative. This can be accomplished by setting the director along the y-axis so that $q_1 < 0$, and setting S_0 large enough so that the inequality holds. This is simulated via the finite element method in [2], and it is found that the configuration quickly blows up.

Indeed, a more general result is proved in [1] which shows that for a fourth-order Landau-de Gennes free energy and $L_3 \neq 0$, a system with arbitrary Dirichlet boundary conditions can be made to have arbitrarily negative free energy. This is not the case with the Maier-Saupe free energy. With this theory, the Lagrange multiplier values Λ diverges to infinity as any of the eigenvalues of Q approach the physically allowed limits. Hence, S_0 is limited by these bounds and so, under appropriate conditions on the elastic constants, one can show that there is a unique minimizer of the Maier-Saupe free energy [2]. For this reason, the theory is able to simulate elastic anisotropy, while the standard Landau-de Gennes theory is not.

3.3 Topological defects

HERE I WANT TO BRIEFLY EXPLAIN WHAT DEFECTS LOOK LIKE AND WHAT THEY ARE

4 Hydrodynamics

The derivation of the time evolution of the system in the preceding section assumed purely thermodynamic interactions. That is, no transfer of mass or corresponding hydrodynamic flow, only transfer of energy and entropy. This is insufficient for many cases, however, as one might imagine flows having a non-negligible effect on molecular alignment. That said, there is yet to be a hydrodynamic theory for the Q-tensor model which is generally accepted by the community. By using general conservation laws of fluid mechanics applied to the director formulation of nematic liquid crystal theory, Ericksen and Leslie were able to derive hydrodynamic equations of a uniaxial nematic liquid crystal system with constant scalar order. However, it happens that for a more general tensorial theory one needs additional contitutive relations in order to produce governing equations.

There have been several attempts at this, including by Beris and Edwards through use of their "dissipation bracket", by Qian and Sheng through methods similar to Ericksen and Leslie but with additional contitutive equations, and by Sonnet and Virga through use of a generalized Rayleigh dissipation factor. All of these models are still poorly characterized and so we, to follow other computational work that has been done in the field, choose the Qian and Sheng formulation. They, however, use a Landau-de Gennes expression for the bulk portion of their free energy while we use the Maier-Saupe expression presented above.

In what follows, we merely quote the hydrodynamic equations and explain several simplifying assumptions that we make upon a first pass. We begin with the generalized (tensorial) force equation:

$$J\ddot{Q} = h + h' \tag{39}$$

Here J is the moment of inertia density (which we will take to be negligible), h is the generalized force from thermodynamics and h' is the viscous generalized force. The generalized force h is given as in section 3 as:

$$h = -\frac{\partial f}{\partial Q} + \nabla \cdot \frac{\partial f}{\partial (\nabla Q)} - \lambda_0 Q : I - \lambda \cdot (\varepsilon : Q) \tag{40}$$

The viscous generalized force is given by:

$$-h' = \tfrac{1}{2}\mu_2 A + \mu_1 N \tag{41}$$

where $A = \frac{1}{2}\left(\nabla v + (\nabla v)^T\right)$ is the symmetric part of the velocity gradient tensor, and $N = dQ/dt + (WQ - QW)$ is the corotational derivative, representing the time rate of change of Q is a frame that rotates with the fluid element. Here $d/dt = \partial/\partial t + \nabla \cdot v$ is the material derivative, and $W = \frac{1}{2}\left(\nabla v - (\nabla v)^T\right)$ is the antisymmetric part of the velocity gradient tensor. To find an expression for the time evolution of Q we plug (41) into (39), and then solve for N:

$$N = \frac{1}{\mu_1}h - \frac{1}{2}\frac{\mu_2}{\mu_1}A \tag{42}$$

Plugging in for N yields:

$$\frac{dQ}{dt} = \frac{1}{\mu_1}h + [Q, W] - \frac{1}{2}\frac{\mu_2}{\mu_1}A \tag{43}$$

with $[Q, W] = QW - WQ$ the commutator.

The flow equation is given by:

$$\rho\frac{dv}{dt} = \nabla \cdot \left(-pI + \sigma^d + \sigma^f + \sigma'\right) \tag{44}$$

with v the velocity, p the pressure, σ^d the stress tensor from distortions in the nematic field, σ^f the stress tensor from external fields (i.e. electric and magnetic), and σ' the viscous stress tensor. This along with the incompressibility condition $\nabla \cdot v = 0$ defines the system. We do not consider external

fields so that $\sigma^f = 0$ and we suppose that flow is steady so that $dv/dt = 0$. The elastic stress is given in terms of the free energy density as:

$$\sigma^d = -\frac{\partial f}{\partial(\nabla Q)} : (\nabla Q)^T \tag{45}$$

The viscous stress tensor is given by:

$$\sigma' = \beta_1 Q\,(Q:A) + \beta_4 A + \beta_5 QA + \beta_6 AQ + \frac{1}{2}\mu_2 N \tag{46}$$
$$- \mu_1 QN + \mu_1 NQ$$

It has been shown that, in configurations of defect annihilation the β_1, β_5, and β_6 terms are negligible, only producing quantitative effects. Additionally, we choose to neglect the μ_1 terms. These do, in fact, produce a qualitative difference in the case of defect annihilation, creating an asymmetry in the trajectory of $+1/2$ and $-1/2$ defects. However, for now we seek to linearize the flow equation so that we only have to solve a much simpler Stoke's system.

These simplifications, along with (42) give the following flow equation:

$$0 = \nabla \cdot \left(-pI + \sigma^d + \beta_4 A + \frac{\mu_2}{2\mu_1} h - \frac{\mu_2^2}{4\mu_1} A \right) \tag{47}$$

Solving for A yields:

$$-2\nabla \cdot A + \frac{1}{\gamma_1}\nabla p = \nabla \cdot \left(\frac{1}{\gamma_1}\sigma^d + \frac{1}{\gamma_2} h \right) \tag{48}$$

with viscosities γ_1 and γ_2 given by:

$$\gamma_1 = \frac{\beta_4}{2} - \frac{\mu_2^2}{8\mu_1}, \quad \gamma_2 = \frac{\mu_1 \beta_4}{\mu_2} - \frac{\mu_2}{4} \tag{49}$$

Hence, equations (43) and (48) comprise our coupled hydrodynamic and thermodynamic system. Note that σ^d and h only depend on Q, so that we have (somewhat artificially) decoupled the right-hand side from flow. As a final note, we explicitly calculate σ^d:

$$\sigma^d = -2L_1 \nabla Q : (\nabla Q)^T - L_2 (\nabla \cdot Q) \cdot (\nabla Q)^T - 2L_3 \left(Q \cdot \left[(\nabla Q) : (\nabla Q)^T \right] \right)^T \tag{50}$$

5 Numerical scheme

To solve these equations numerically, we first discretize in time by using a semi-implicit method which leverages convexity of several terms to increase the convergence rate. Given the semi-implicit time-stepping scheme, as well as the nonlinearity of the equations, we must use Newton's method to update the time step. Spatial discretization is done by introducing a weak form of the equations, and then using a finite element method to solve each of the couple equations. In the course of setting up the finite element system, we will have need of inverting the Lagrange multiplier Λ and we will also need to find the Jacobian of that mapping, due to the overall Newton's method imposed on the implicit time-stepping scheme. This must be done efficiently, as it happens at every quadrature point in the finite element mesh several times per time-step. We detail each of these steps below.

5.1 Nondimensionalization

We begin by nondimensionalizing the generalized force h, whose explicit expression is exactly the right-hand side of (34). To do this, we introduce a length-scale ξ and write gradients as derivatives

11

with respect to the nondimensional length $\bar{x} = x/\xi$. Additionally, we may divide by the energy density nk_BT:

$$\frac{h}{nk_BT} = \frac{2\alpha}{nk_BT} - \Lambda + \frac{2L_1}{nk_BT\xi^2}\nabla^2 Q \tag{51}$$

$$+ \frac{L_2}{nk_BT\xi^2}\left(\nabla(\nabla\cdot Q) + [\nabla(\nabla\cdot Q)]^T - \tfrac{2}{3}(\nabla\cdot(\nabla\cdot Q))I\right)$$

$$+ \frac{L_3}{nk_BT\xi^2}\left(2\nabla\cdot(Q\cdot\nabla Q) - (\nabla Q):(\nabla Q)^T + \tfrac{1}{3}|\nabla Q|^2 I\right)$$

Now we define the following quantities:

$$\xi = \sqrt{\frac{2L_1}{nk_BT}}, \quad \bar{\alpha} = \frac{2\alpha}{nk_BT}, \quad \bar{h} = \frac{h}{nk_BT}, \quad \overline{L_2} = \frac{L_2}{L_1}, \quad \overline{L_3} = \frac{L_3}{L_1} \tag{52}$$

Plugging in and dropping the overlines for brevity, this yields:

$$h = \alpha Q - \Lambda + \nabla^2 Q + L_2\,E_2(Q,\nabla Q) + L_3\,E_3(Q,\nabla Q) \tag{53}$$

with anisotropic elastic terms given by:

$$E_2(Q,\nabla Q) = \tfrac{1}{2}\left[\nabla(\nabla\cdot Q) + [\nabla(\nabla\cdot Q)]^T\right] - \tfrac{1}{3}(\nabla\cdot(\nabla\cdot Q))I \tag{54}$$

$$E_3(Q,\nabla Q) = \nabla\cdot(Q\cdot\nabla Q) - \tfrac{1}{2}(\nabla Q):(\nabla Q)^T + \tfrac{1}{6}|\nabla Q|^2 I \tag{55}$$

To nondimensionalize (43), we first note that A and W have dimensions of inverse time, because the characteristic length scale ξ cancels between the gradient and the velocity. Hence, we may introduce a characteristic time τ as:

$$\frac{1}{\tau}\frac{dQ}{d\bar{t}} = \frac{nk_BT}{\mu_1}\bar{h} + \frac{1}{\tau}[Q,W] - \frac{1}{2}\frac{\mu_2}{\mu_1}\frac{1}{\tau} \tag{56}$$

Given this, we make the following definitions:

$$\tau = \frac{\mu_1}{nk_BT}, \quad \gamma = -\frac{1}{2}\frac{\mu_2}{\mu_1} \tag{57}$$

Note that μ_2/μ_1 is typically negative so that the so-called flow-alignment parameter γ is positive. Dropping overlines, this gives:

$$\frac{dQ}{dt} = h + [Q,W] + \gamma A \tag{58}$$

For the Stokes equation, we begin by nondimensionalizing the elastic stress tensor. Substituting the characteristic length, we end up with:

$$\bar{\sigma}^d = -\nabla Q:(\nabla Q)^T - \tfrac{1}{2}\overline{L}_2(\nabla\cdot Q)\cdot(\nabla Q)^T - \overline{L}_3\left(Q\cdot\left[(\nabla Q):(\nabla Q)^T\right]\right) \tag{59}$$

with:

$$\sigma^d = \bar{\sigma}^d nk_BT \tag{60}$$

With this, the flow equation reads:

$$-2\frac{1}{\tau\xi}\nabla\cdot A + \frac{1}{\gamma_1}\frac{\eta}{\xi}\nabla p = \frac{1}{\xi}\nabla\cdot\left(\frac{1}{\gamma_1}nk_BT\sigma^d + \frac{1}{\gamma_2}nk_BTh\right) \tag{61}$$

Here η is a dimensional parameter associated with p. Multiplying through by $\xi\tau$, and then using the definition of τ we find:

$$-2\nabla\cdot A + \nabla p = \nabla\cdot\left(\zeta_1\sigma^d + \zeta_2 h\right) \tag{62}$$

where we have taken:

$$\eta = \gamma_1/\tau, \quad \zeta_1 = \left(\frac{1}{2}\frac{\beta_4}{\mu_1} - \frac{1}{8}\left(\frac{\mu_2}{\mu_1}\right)^2\right)^{-1}, \quad \zeta_2 = \left(\frac{\beta_4}{\mu_2} - \frac{1}{4}\frac{\mu_2}{\mu_1}\right)^{-1} \tag{63}$$

Hence, the remaining parameters in the system are: the interaction parameter α which is controlled by the temperature; the anisotropic elasticities L_2 and L_3; the flow-alignment parameter γ which controls the nematic's tendency to align along the direction of flow; and the two viscosity parameters ζ_1 and ζ_2 which control the relative weight with which generalized force and elastic stress tensor affect the flow configuration.

5.2 Discretization of Q-tensor equation

Given that the Q-tensor is traceless and symmetric, we may write it in terms of its degrees of freedom as:

$$Q = \begin{bmatrix} Q_1 & Q_2 & Q_3 \\ Q_2 & Q_4 & Q_5 \\ Q_3 & Q_5 & -(Q_1 + Q_4) \end{bmatrix} \tag{64}$$

and collect those degrees of freedom into a five-component vector, q:

$$q = \begin{bmatrix} Q_1 \\ Q_2 \\ Q_3 \\ Q_4 \\ Q_5 \end{bmatrix} \tag{65}$$

There are several other traceless and symmetric quantities which are functions of Q (and therefore may be written as vector functions of q), but which require tensor contraction operations, and can thus not simply be notated as vector operations on q. In an attempt to compartmentalize cumbersome notation, we collect the degrees of freedom of these traceless, symmetric tensors into corresponding vectors, and write them as functions of the vector q to get:

$$\Lambda(Q) \to \lambda(q), \quad E_2(Q, \nabla Q) \to e_2(q, \nabla q), \quad E_3(Q, \nabla Q) \to e_3(q, \nabla q), \quad [Q, W] \to c(q), \quad A \to a \tag{66}$$

The details of calculating these vector quantities in terms of q are relegated to the appendices.

Now, for a purely thermodynamic system one can show that the free energy corresponding to the molecular interaction energy (the α term), is convex. Additionally, the sum of the elastic and Lagrange multiplier free energies are convex. Hence, one may adopt a convex splitting scheme which allows one to use a much larger time-step. For this, we treat the molecular interaction energy explicitly, and all other terms implicitly so that the time-discretized evolution equation reads:

$$\frac{q - q_0}{\delta t} + v \cdot \nabla q = \alpha q_0 - \lambda(q) + \nabla^2 q + L_2\, e_2(q, \nabla q) + L_3\, e_3(q, \nabla q) + c(q) + \gamma a \tag{67}$$

where q is the configuration at the current time-step, q_0 is the configuration at the previous time-step, and δt is the step size. Given that this is a nonlinear equation which we seek to solve via a finite element method, we must use the Newton-Rhapson method to linearize. To that end, we define a vector residual:

$$\mathcal{R}(q^n) = q^n + v \cdot \nabla q^n - (1 + \delta t\, \alpha)q_0 - \delta t \left(-\lambda(q^n) + \nabla^2 q^n + L_2\, e_2(q^n, \nabla q^n) + L_3\, e_3(q^n, \nabla q^n) + c(q^n) + \gamma a\right) \tag{68}$$

where q^n is the value of q for the nth Newton iteration. Then the iterative method reads:

$$\mathcal{R}'(q^n)\delta q^n = -\mathcal{R}(q^n)$$
$$q^{n+1} = q^n + \alpha_0 \delta q^n \tag{69}$$

13

with $\mathcal{R}'$ the Gateaux derivative of the residual, and δq^n the variation of q which must be solved for at each time step. $\alpha_0 < 1$ is a step size that can be made smaller for a system for which the convergence is more sensitive. Explicitly, the Jacobian $\mathcal{R}'$ reads:

$$\mathcal{R}'\delta q^n = \delta q^n + v \cdot \nabla \delta q^n - \delta t \left[- \left(\frac{\partial \lambda}{\partial q} \right)\bigg|_{q^n} \delta q^n + \nabla^2 \delta q^n \right. \tag{70}$$

$$\left. + L_2 e_2'(q^n, \nabla q^n)\, \delta q^n + L_3 e_3'(q^n, \nabla q^n)\, \delta q^n + c'(q^n)\, \delta q^n \right]$$

Here e_2' and e_3' are linear operators which depend on the configuration at the last Newton iteration, and contain differential operators. c' is a matrix whose values only depend on q^n.

We now cast this linear equation in its weak form by taking an inner product with an arbitrary (vector) test function φ:

$$\langle \varphi, \mathcal{R}'\delta q \rangle = -\langle \varphi, \mathcal{R} \rangle \tag{71}$$

where here we define the inner product as:

$$\langle f, g \rangle = \int_\Omega f \cdot g \tag{72}$$

for the domain Ω. To recast this as a discrete problem, we dictate that (71) must be satisfied for some finite-dimensional subspace of the space of test functions with basis ϕ_i. Further, we represent the solution δq^n (approximately) as a linear combination of these basis elements:

$$\delta q^n = \sum_i \delta q_i^n \varphi_i \tag{73}$$

If we plug this approximation into (71) and integrate by parts, we get an equation with the following form:

$$A_{ij}^n \delta q_j^n = b_i^n \tag{74}$$

with

$$A_{ij}^n = \langle \varphi_i, \varphi_j \rangle + \langle \varphi_i, v \cdot \nabla \varphi_j \rangle - \delta t \left[- \left\langle \varphi_i, \left(\frac{\partial \lambda}{\partial q} \right) \varphi_j \right\rangle - \langle \nabla \varphi_i, \nabla \varphi_j \rangle \right. \tag{75}$$

$$\left. + L_2 \langle \varphi_i, e_2' \varphi_j \rangle + L_3 \langle \varphi_i, e_3' \varphi_j \rangle + \langle \varphi_i, c' \varphi_j \rangle \right]$$

and

$$b_i = \langle \varphi_i, q^n \rangle + \langle \varphi_i, v \cdot \nabla q^n \rangle - (1 + \delta t\, \alpha)\langle \varphi_i, q_0 \rangle \tag{76}$$

$$- \delta t \left[-\langle \varphi_i, \lambda(q^n) \rangle - \langle \nabla \varphi_i, \nabla q^n \rangle + L_2 \langle \varphi_i, e_2(q^n) \rangle \right.$$

$$\left. + L_3 \langle \varphi_i, e_3(q^n) \rangle + \langle \varphi_i, c(q^n) \rangle + \gamma \langle \varphi_i, a(v) \rangle \right]$$

Here we have, for the isotropic elasticity terms, integrated by parts:

$$\langle \varphi_i, \nabla^2 \varphi_j \rangle = \langle \varphi_i, n \cdot \nabla \varphi_j \rangle_{\partial\Omega} + \langle \nabla \varphi_i, \nabla \varphi_j \rangle \tag{77}$$

where n is the unit vector normal to the boundary $\partial\Omega$, and the corresponding inner product is integrated over the boundary. For now we assume either Dirichlet or zero-valued Neumann conditions. In the former case, the test functions φ_i come from the space tangent to the solution space so that they are zero on the boundary. In the latter case, the normal derivative is zero. In both cases, the boundary term vanishes. For more general boundary-conditions (nonzero Neumann or mixed), we just end up with another term on the right-hand side which can be calculated from the values of the normal derivative prescribed at the boundary.

5.3 Discretization of the Stokes equation

Given that the simplified hydrodynamic model gives the flow velocity in the form of a typical Stoke's equation, the discretization is somewhat standard. We first collect the equations into a single vector equation:

$$\begin{pmatrix} -2\nabla \cdot A(v) + \nabla p \\ -\nabla \cdot v \end{pmatrix} = \begin{pmatrix} \nabla \cdot \left(\zeta_1 \sigma^d + \zeta_2 h \right) \\ 0 \end{pmatrix} \tag{78}$$

We then dot with a vector set of test equations $\begin{pmatrix} u & q \end{pmatrix}^T$ with u in the space of velocity functions, and q in the space of pressure functions. This yields:

$$\langle u, -2\nabla \cdot A(v) + \nabla p \rangle - \langle q, \nabla \cdot v \rangle = \langle u, \nabla \cdot \left(\zeta_1 \sigma^d + \zeta_2 h \right) \rangle \tag{79}$$

Now we may use the divergence theorem to integrate by parts, and also note that:

$$\begin{aligned} \tfrac{1}{2} \left(\nabla u \right) : \left(\nabla v + (\nabla v)^T \right) &= \tfrac{1}{2} \left(\partial_i u_j \right) \left(\partial_j v_i + \partial_i v_j \right) \\ &= \tfrac{1}{4} \left[\left(\partial_i u_j \right) \left(\partial_j v_i + \partial_i v_j \right) + \left(\partial_j u_i \right) \left(\partial_i v_j + \partial_j v_i \right) \right] \\ &= A(u) : A(v) \end{aligned} \tag{80}$$

where for the second term in the second equality we have relabeled $i \to j$, $j \to i$. Given this, the weak form of our equation reads:

$$2\langle A(u), A(v) \rangle - \langle \nabla \cdot u, p \rangle - \langle q, \nabla \cdot v \rangle = -\langle \nabla u, \zeta_1 \sigma^d + \zeta_2 h \rangle \tag{81}$$

Here we have chosen no slip boundary conditions so that the boundary terms from the weak form go to zero.

To discretize, we choose a finite test function basis $\varphi_i = \begin{pmatrix} \varphi_{i,v} & \varphi_{i,p} \end{pmatrix}$ to act as our test functions as well as a basis for our solution. The equations in the form above happen to be a symmetric saddle-point problem so that, in order to have a unique solution, the finite-dimensional solution space must satisfy the Ladyzhenskaya-Babuska-Brezzi (LBB) conditions. For our purposes it suffices to choose Lagrange (piece-wise polynomial) elements so that the pressure part of the solution $\varphi_{i,p}$ is represented by elements of degree d, and the velocity solution $\varphi_{i,v}$ is represented by elements of degree $d + 1$. This then becomes a matrix inversion problem with matrix

$$A_{ij} = 2\langle A(\varphi_{i,v}), A(\varphi_{j,v}) \rangle - \langle \nabla \cdot \varphi_{i,v}, \varphi_{j,p} \rangle - \langle \varphi_{i,p}, \nabla \cdot \varphi_{j,v} \rangle \tag{82}$$

and right-hand side:

$$b_i = -\langle \nabla \varphi_{i,v}, \zeta_1 \sigma^d + \zeta_2 h \rangle \tag{83}$$

5.4 Algorithm details

To initialize the system, we project a nematic configuration onto the finite element solution space of the q-vector. This configuration typically is some arrangement of topological defects. We then iterate forward in time several steps ($\sim 20\,\tau$) to let it relax before introducing hydrodynamics. We do this because the analytic expressions for topological defects typically only dictate the director angle at each point in space, and so there is a singularity at the defect cores, resulting in large gradients and therefore large velocity fields. By letting the (largely diffusive) system relax, the scalar order parameter S decreases near the defect cores so that the Q-tensor configuration is smoother. As explained above, to step in time we must iterate a Newton-Rhapson equation until some tolerance is reached for the norm of the residual $\mathcal{R}$. For the initial configuration, we fix $v = 0$.

Once the system is initialized and relaxed, we introduce hydrodynamics. Given that we are solving two simultaneous equations which we have artificially decoupled, we iterate in time as follows: the first Newton iteration of the Q-configuration q^1 is solved using the velocity field v^0 from

the last time step. Then we solve for the velocity field v^1 corresponding to q^1. Given v^1 we may solve for the q-configuration at the next Newton iteration, q^2. We continue back and forth until the residual $\mathcal{R}$ reaches some tolerance. Given that the dependence of v on q is not taken into account when computing the Jacobian of the residual $\mathcal{R}'$, it is necessary to take a much smaller step for each Newton iteration: we choose $\alpha_0 = \frac{1}{2}$.

To solve the matrix equation for δq, we use an iterative GMRES solver. An iterative solver is preferable over a direct solver in order to save on memory costs, as well as operation scaling: for GMRES, only vector-vector and matrix-vector operations are necessary so that, for a sparse matrix as in this problem, each iteration scales linearly with the number of degrees of freedom. Additionally, in a problem simulating only diffusion (no hydrodynamics) we have implemented the BoomerAMG algebraic multigrid solver to precondition the matrices. This method has the added benefit of keeping the number of GMRES iterations constant so that the entire solver scales linearly. Further, both of these solvers can run in a distributed fashion so that the program can be parallelized to thousands of processors.

To solve the Stoke's equation, we borrow largely from (cite deal.II). Here they use a Schur complement method to decouple the velocity and pressure equations into two symmetric matrix equations. The matrix equation is then solved by using a mix of direct solvers, and iterative Conjugate Gradient solvers. See (cite deal.II) for details. Note also that the algebraic multigrid method can be used as a preconditioner for this system, thus allowing it to be highly scalable via parallelization.

This algorithm is implemented in $C++$ using the deal.II finite element library for the standard steps: mesh-generation, finite element basis functions, projection onto finite element space, building finite element matrices, distributing boundary constraints, solving matrix inversion problems, and several other operations. The project is open source and freely available at (cite github repo).

5.5   Inverting the Lagrange multiplier function

To find a solution, we must numerically calculate both the Lagrange multiplier λ, as well as its Jacobian $\partial \lambda / \partial q$. We do this by using a Newton-Rhapson method, with a residual given by (25). In principle, the residual would be a five-component vector corresponding to the five degrees of freedom of Q. However, that would require calculating an integral around the sphere for each of the five components. Further, the Jacobian of the residual (a 5×5 matrix) requires 60 total integrals. These must be computed numerically, and so for a Lebedev quadrature scheme with any reasonable number of points, would become the dominant computational cost of a program.

To circumvent this, we first note that Q and Λ are simultaneously diagonalized. For a diagonalized traceless tensor there are only two degrees of freedom, and so the corresponding residual is two components and its Jacobian is a 2×2 matrix. This corresponds to a total of six integrals around the sphere. Hence, we may first diagonalize Q and record the corresponding rotation matrix, compute the two degrees of freedom of the diagonalized Λ-tensor, and then find Λ in the original frame by computing the inverse rotation. However, we also seek to calculate $\partial \lambda / \partial q$. In the case described above, where we calculate the full five degrees of freedom with Newton's method, that quantity is just the inverse of the residual's Jacobian. For this, we construct a commutative diagram of the relevant mappings.

Here ϕ maps the degrees of freedom of the traceless, symmetric tensors to entries in a vector in $\mathbb{R}^5$, diag is the diagonalization procedure which is unique on the space of symmetric matrices, ψ maps the degrees of freedom of the diagonalized traceless, symmetric tensors to $\mathbb{R}^2$ and degrees of freedom of rotation matrices to $\mathbb{R}^5$ via some means. For numerical stability we use unit quaternions to represent the rotations, keeping in mind that it does not matter that they double-cover $SO(3)$ so long as we consistently map to a single half. Additionally, Λ is the mapping which takes the Q-tensor to it's unique Lagrange multiplier, and λ is the same for the vector representation. Given

$$
\begin{array}{ccc}
D^{Tr} \times SO(3) & \xrightarrow{\ \Lambda \times I\ } & D^{Tr} \times SO(3) \\
\end{array}
$$

$$
\begin{array}{ccccc}
 & \text{diag}\nearrow & \big\downarrow \psi & & \text{diag}\nearrow \\
S^{Tr} & \xrightarrow{\qquad \Lambda \qquad} & & S^{Tr} & \big\downarrow \psi \\
\big\downarrow \phi & \mathbb{R}^2 \times \mathbb{R}^3 & \xrightarrow{\lambda \times I} & \big\downarrow \phi & \longrightarrow \mathbb{R}^2 \times \mathbb{R}^3 \\
\mathbb{R}^5 & \xrightarrow{\qquad \lambda \qquad} & & \mathbb{R}^5 &
\end{array}
$$

all this, we may write λ as:

$$
\lambda = \left(\phi \circ \mathrm{diag}^{-1} \circ \psi^{-1}\right) \circ (\lambda \times I) \circ \left(\psi \circ \mathrm{diag} \circ \phi^{-1}\right) \tag{84}
$$

Each mapping in parentheses is just a mapping on $\mathbb{R}^5$ and so we may compute them numerically. The chain rule then gives:

$$
d\lambda = d\left(\phi \circ \mathrm{diag}^{-1} \circ \psi^{-1}\right) \cdot (d\lambda \times I) \cdot d\left(\psi \circ \mathrm{diag} \circ \phi^{-1}\right) \tag{85}
$$

Hence, to find the Jacobian of λ it suffices to find the Jacobians of the diagonalizing and inverse diagonalizing mappings, as well as the Jacobian of λ in the reduced case.

It is not possible to find a closed analytic expression for the diagonalization of a 3×3 matrix which is numerically stable, and so we cannot compute a Jacobian for these mappings analytically. However, automatic differentiation affords us a way to compute the derivatives of these mappings using one of the many numerically-stable diagonalization schemes, such as the Jacobi method, or the QL method with implicit shifts. Computing the derivatives only adds a small factor (roughly two here) to the number of computations. Finally, diagonalizing these matrices introduces further symmetry into the spherical integrals since only factors of x^2, y^2 and z^2 appear. In this case we only need to integrate over the positive octant, which reduces the number of quadrature points by another factor of eight.

6 Comparison with previous results

6.1 Verification of thermodynamics

As a first test for the code, we verify the relaxation of a prototypical configuration with previously published results. For simplicity, we choose an isotropic system ($L_2 = L_3 = 0$) without hydrodynamics $v = 0$ in two dimensions. The nematic configuration is a $+1/2$ defect with scalar order parameter $S = 0.6715$. Explicitly, the initial Q-tensor field reads:

$$
Q = \frac{S}{2} \begin{bmatrix} \frac{1}{3} + \cos(\theta) & \sin(\theta) & 0 \\ \sin(\theta) & \frac{1}{3} - \cos(\theta) & 0 \\ 0 & 0 & -\frac{2}{3} \end{bmatrix} \tag{86}
$$

where θ is the polar coordinate angle. The boundaries of the domain are fixed at these values (i.e. we use Dirichlet conditions). The system size is $\frac{10}{\sqrt{2}} \times \frac{10}{\sqrt{2}}$ in units of the characteristic length ξ, and the finite element mesh is a 256×256 gridpoint square composed of quadrilaterals (in fact squares in this case). To relax the system, we have run Newton's method to make $\partial q/\partial t = 0$, though we could have just as easily iterated in time via the semi-implicit method until the system does not change appreciably between time steps. Indeed, this is what the code in (reference Cody) does, which should give the same relaxed configuration. One other difference between the simulation presented
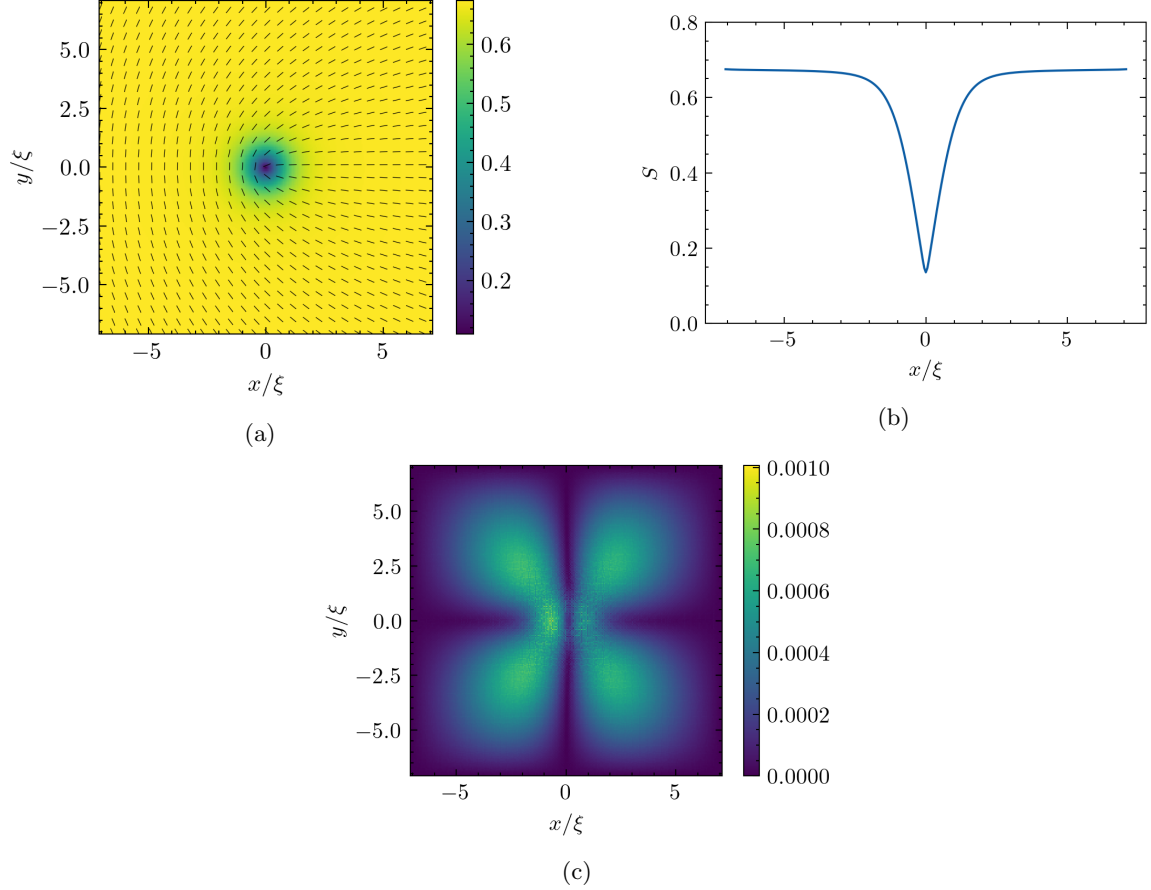
(a)

(b)

(c)

Figure 5: Results from the relaxation of a +1/2 defect. Here (a) is a plot of the defect with dashes representing the director orientation and color scheme representing the scalar order parameter S, (b) is a cross-section of S horizontally through the middle of the defect, and (c) is the vector norm of the difference between the calculated configuration and a reference configuration produced by code from (reference Cody) $|q - q_{\text{ref}}|$.

here and the reference code is that the latter uses triangles for cells, and hence uses a somewhat different mesh.

The configuration is shown in 5a with a cross-section of the scalar order parameter S through the defect shown in 5b. As expected, S is symmetric about the center, and the defect sizing is on the order of the characteristic length. Further, in the defect core S decreases linearly until it reaches the center.

As a final check we can plot the vector norm of the difference between this configuration and one generated by code used in (reference Cody's paper). In 5c we see take the fluctuations in the center to be numerical noise, given that they happen on the order of pixels. Further, the maximal difference is approximately 1% of the total vector norm. Given the different discretizations of the problem (simplices vs quadrilaterals) we take this to be a confirmation of the efficacy of the program.

6.2 Verification of hydrodynamics

To verify the hydrodynamic component of the code, we consider a two-dimensional system of one +1/2 and one −1/2 defect pointing away from one another, as in 6a. We may then – after having

relaxed the configuration as described above – calculate the hydrodynamic flows arising from each of the terms in (62) and compare them to the flows found in (reference Zumer).

Once again we take the isotropic elasticity approximation because the flows that we are interested in comparing to use a Landau-de Gennes free energy, and thus are restricted to the isotropic approximation. The system size here is $\frac{1,400}{3} \times \frac{1,400}{3}$ in units of ξ with outer mesh size 256×256 grid points. The defects, themselves a distance $70\,\xi$ apart, live in a central region of size $\frac{280}{3} \times \frac{280}{3}$ for which the grid has been refined once more. That is, the grid-spacing is halved in the central region. In all of the plots that follow, only the central region is shown.
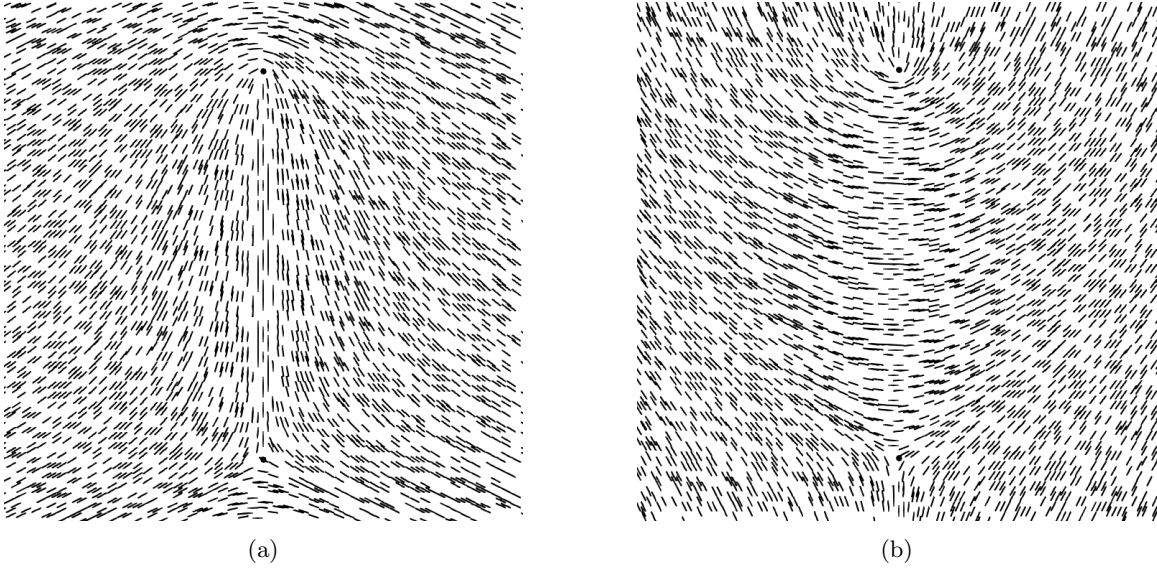

(a) (b)

Figure 6: Schematic representation of the two-defect configurations, with dashes corresponding to the nematic-director angle at that point. These two isomorphs differ by a $\pi/2$ global director rotation, and so any term in the free energy invariant under that transformation treats these configurations identically. Note that (a) corresponds to the defects pointing *away* from one another (the $+1/2$ defect moves like a comet) and (b) corresponds to the defects pointing *towards* one another.

In our linearized approximation to the hydrodynamic equations, there are three contributions from the nematic configuration to the flow: the β_4 and μ_2 viscosity terms, as well as the elastic terms arising from the elastic stress tensor. We consider the flows arising from the μ_2 and elastic terms (always keeping the β_4 terms present), and compare them qualitatively to those from (reference Zumer).

For the flow due only to the elastic stress tensor, we note that both configurations contain four vortices, and that the flow direction is such that the defects are pushed toward one another. The vortex centers in our configuration are further from the center of the domain, likely due to different bulk free energy parameters or to the difference in definition of the characteristic length. Additionally, the configuration is symmetric about the two defects. This can be understood, as described in (ref Zumer), by the transformation which turns the $+1/2$ and $-1/2$ defects into one another $Q_{xy} \to -Q_{xy}$. Because the isotropic elastic stress tensor is insensitive to this change, the resulting flow configuration is symmetric between the two.

The flow due to the μ_2 term, by contrast, is not symmetric about the defects, and in fact the transformation described above has no definite symmetry properties with respect to N. As a result, there is a slight asymmetry in the shape of the vortices around each defect. In any case, we see six vortices instead of four, moving in directions that are consistent with Zumer's results.

Finally, for the flow including all terms we notice significant differences between the two configurations. This is due to the fact that we have neglected the μ_1 viscous terms which, at the

19

(a) all terms

(b) elastic term

(c) μ_2 term

(d) all terms, reference configuration

(e) elastic terms, reference configuration

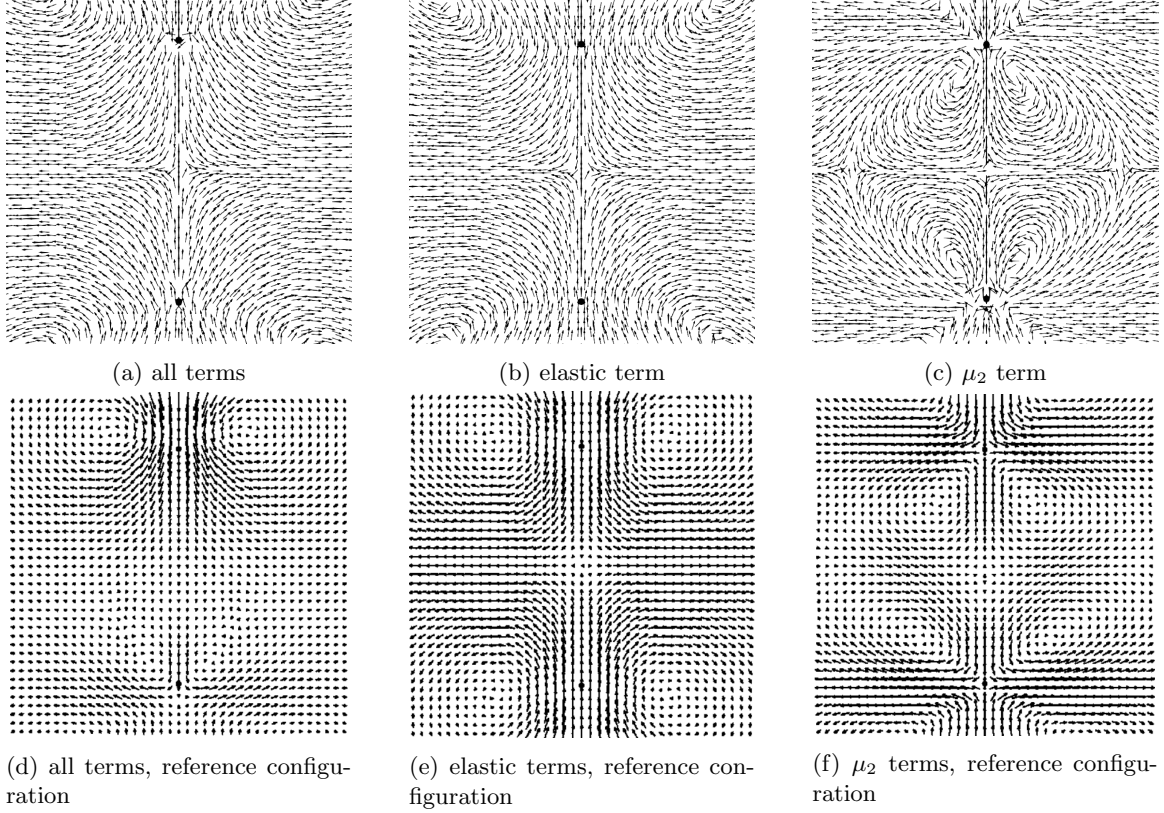(f) μ_2 terms, reference configuration

Figure 7: Instantaneous flow configurations arising from the nematic configuration pictured in 6a. Figures (a)-(c) are our configurations produced by solving (62), while (d)-(e) are reference configurations from (reference Zumer). Figure (b) considers only the elastic stress tensor, (c) considers only the μ_2 term, and (a) contains both. Figure (e) considers only elastic terms, (f) considers μ_2 terms, while (d) considers elastic and all of the viscous terms described in (46). Note that all of the configurations consider the β_4 viscous term.

location of the $+1/2$ defect point *toward* the $-1/2$ defect, and and at the location of the $-1/2$ defect point *away* from the $+1/2$ defect. Thus, at the $-1/2$ defect location the flows from the μ_1 viscous term and the elastic stress tensor cancel out, giving a large asymmetry in the flow velocities at each of the defects. In our case, the elastic flow configuration largely dominates and so the total flow configuration only has four vortices.

7 Intended research

7.1 Backflows from two-defect configuration

In the classical work by Svensek and Zumer referenced above, they investigate the effect of backflows on the trajectories of two defects of opposite charge. However, they use a Landau-de Gennes bulk free energy and are thus limited to the single-constant isotropic elasticity approximation. We seek to simulate the same system, but with anisotropy between the splay and bend elastic modes.

In their investigation, they consider two isomorphs, one in which the the defects are pointing towards each other, and one away (reference figure). For isotropic elasticity, the free energy is unaffected by a rotation of the director by some fixed phase everywhere in space. A rotation by $\pi/2$ turns one isomorph into the other, and so the defect motion should be the same in either case.

However, given that the region in between the defects in isomorph (a) is dominated by splay, while the region between the defects in isomorph (b) is dominated by bend, it is expected that anisotropy will cause different annihilation trajectories between the two scenarios. Additionally, for isotropic elasticity the two defects experience symmetric, parabolic-in-time trajectories and annihilate in the center of their initial separation. This is because, as mentioned above, the $Q_{xy} \rightarrow -Q_{xy}$ transformation turns one into the other. Given that anisotropic elasticity causes the defects to locally relax into different shapes – U-like for splay-dominated, V-like for bend-dominated – this symmetry no longer holds and so we expect the trajectories to be asymmetric.

7.2   Three-dimensional configurations

In three dimensions, instead of only point defects we may additionally find line-defects. For the simplest case, a so-called wedge disclination may be constructed by taking a two-dimensional defect like those shown above and extending it to be uniform in the third dimension. However, in this case the directors may point in the third dimension and so for a purely $+1/2$ defect manufactured as described, along a plane perpendicular to the defect line one may continuously rotate the director field to a twist defect, and then to a $-1/2$ defect. Hence, there is no purely topological difference between $+1/2$ and $-1/2$ defects in three dimensions. Given this, there is some question as to whether there is a persistent asymmetry in the backflows produced by wedge disclinations as demonstrated by (reference Zumer) in two dimensions. In recent measurements it has been shown that pairs of disclinations do follow the same parabolic-in-time annihilation pattern shown in (reference Zumer) in the case without backflow, and so it is speculated that the wedge defects undergo the transformation described above so that they both become twist defects. This is true no matter the defect configuration (straight and parallel vs. curved more generally), though certain theories predict it should only be true for straight disclinations. It has been argued that the mechanism for transformation into twist disclinations is mediated by anisotropic elasticity, and so we hope to use our computational scheme to study the details of three-dimensional defect dynamics in the midst of anisotropy.

8   Conclusion

In this paper we have given an overview of the theory of nematic liquid crystals, as well as a modified model which couples thermodynamics and hydrodynamics. Additionally, we have detailed a computational implementation which can simulate the dynamics of a variety of liquid crystal systems. We have shown that, in the absence of hydrodynamics, the relaxation of a $+1/2$ defect is the same as in previously published work, modulo numerical noise. Further, we have computed the flows associated with a $+1/2$, $-1/2$ defect pair, and shown that they qualitatively match with previous results. Finally, we indicate several areas where an investigation of defect dynamics with anisotropic elasticity may yield fruitful results: namely for defect annihilation for a pair of $+1/2$ and $-1/2$ defects in two dimensions, and for different configurations of wedge disclination annihilations in three dimensions.

References

[1] John M. Ball and Apala Majumdar. Nematic Liquid Crystals: From Maier-Saupe to a Continuum Theory. *Molecular Crystals and Liquid Crystals*, 525(1):1–11, July 2010.

[2] Cody D. Schimming, Jorge Viñals, and Shawn W. Walker. Numerical method for the equilibrium configurations of a Maier-Saupe bulk potential in a Q-tensor model of an anisotropic nematic liquid crystal. *Journal of Computational Physics*, 441:110441, September 2021.

[3] Rui Zhang, Nitin Kumar, Jennifer L. Ross, Margaret L. Gardel, and Juan J. de Pablo. Interplay of structure, elasticity, and dynamics in actin-based nematic materials. *Proceedings of the National Academy of Sciences*, 115(2), January 2018.